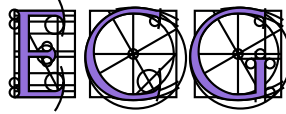


**ECG**  
*IST-2000-26473*  
Effective Computational Geometry for Curves and Surfaces



ECG Technical Report No. : *ECG-TR-244104-01*

*Provably Good Surface Sampling and Approximation*

Steve Oudot

Jean-Daniel Boissonnat

Deliverable: 24 41 04 (item 01)  
Site: INRIA  
Month: 24



Project funded by the European Community  
under the “Information Society Technologies”  
Programme (1998–2002)





## Abstract

We present an algorithm for meshing surfaces that is a simple adaptation of a greedy “farthest point” technique proposed by Chew. Given a surface  $S$ , it progressively adds points on  $S$  and updates the 3-dimensional Delaunay triangulation of the points. The method is very simple and works in  $3d$ -space without requiring to parameterize the surface. Taking advantage of recent results on the restricted Delaunay triangulation, we prove that the algorithm can generate good samples on  $S$  as well as triangulated surfaces that approximate  $S$ . More precisely, we show that the restricted Delaunay triangulation  $\text{Del}_{|S}$  of the points has the same topology type as  $S$ , that the Hausdorff distance between  $\text{Del}_{|S}$  and  $S$  can be made arbitrarily small, and that we can bound the aspect ratio of the facets of  $\text{Del}_{|S}$ . The algorithm has been implemented and we report on experimental results that provide evidence that it is very effective in practice. We present results on implicit surfaces, on CSG models and on polyhedra. Although most of our theoretical results are given for smooth closed surfaces, the method is quite robust in handling smooth surfaces with boundaries, and even non-smooth surfaces.

Partially supported by the IST Programme of the EU as a Shared-cost RTD (FET Open) Project under Contract No IST-2000-26473 (ECG - Effective Computational Geometry for Curves and Surfaces)

## 1 Introduction

A lot of applications dealing with surfaces require the use of discretized geometric models for fast and efficient computation. For instance, in computer graphics, most of the rendering techniques work on polyhedral approximations of the objects rather than on the objects themselves. In the same way, numerical simulations based on finite elements rely on discrete descriptions. Therefore it is an important issue to produce meshes to approximate geometric models. Here we deal exclusively with simplicial meshes and consider the following problem:

*Given a known 2-manifold  $S$  embedded in  $\mathbb{R}^3$ , a metric  $L$  and a constant  $\epsilon > 0$ , build a triangulated 2-manifold  $P$  with a minimum number of vertices, such that  $S$  and  $P$  are homeomorphic and  $L(S, P) \leq \epsilon$ .*

A discrete version of this problem has been shown to be *NP*-hard [1]. To our knowledge, it is still an open question to approximate the solution to this problem for general surfaces in a both efficient and provably correct manner. The choice of the metric is an issue by itself. Hausdorff distance is a first candidate, but we would like to control also differential quantities like normals or curvatures, as well as the aspect ratio of the facets.

### Previous work

Previous work on surface meshing resorts to two types of techniques: grids and particles systems. The former type relies on a tessellation of  $3d$ -space [18, 7]. A polygonal approximation of the surface is computed inside each cell. Its vertices are located where the function has opposite signs. A global approximation is obtained by gluing all the polygonal patches together. This approach yields volume-based approximations. However, the topology of the surface is not always preserved, although methods have been proposed to guarantee the topological consistency of the result [7]. In addition, the point distribution is hardly controllable.

Particles methods make sets of particles migrate along the surface [23, 25, 9], according to diffusion equations. The connectivity between the points is built by various means which usually do not guarantee the topology of the output mesh. A step forward has been done by Hart and Stander [14], who proposed to use Morse theory to capture the correct topology. Unfortunately, the method is mostly heuristic and the authors do not provide a proof of correctness of their algorithm.

A lot of work has been recently devoted to the problem of remeshing polyhedral surfaces. Although this issue is quite different from the previous one, our method can be used for both problems. We briefly survey prominent remeshing techniques. Particles methods have been proposed [24], but the time required to compute the solution of the equation of diffusion makes them less efficient than methods based on heuristics. The latter combine mesh simplification [15] and vertex optimization, and they allow to control the point density [13, 17]. Another class of algorithms is based on global parameterization [16, 2], which allows quick mesh generation. But the use of a global parameterization requires to cut the surface into patches, which produces artificial 1-manifolds – from the cut-graph – that are visible in the final mesh.

## Contributions

In this paper, we revisit a greedy “farthest point” technique, which was originally proposed by Chew [8] for the mesh refinement problem. Given a 2-manifold  $S$  embedded in  $\mathbb{R}^3$  and a mesh  $M$  whose vertices are on  $S$ , the mesh refinement problem consists in inserting new points of  $S$  as vertices of  $M$  and rebuilding the connectivity accordingly, so that all facets of  $M$  meet some criterion. This problem has been well-studied in the planar case and provably good methods based on the Delaunay triangulation have been proposed [21, 22]. These methods allow to control the size and the shape of the triangles. Chew’s algorithm uses a variant of the Delaunay triangulation for surfaces. Our main contributions are the following:

- we give a variant of Chew’s algorithm that relies on the restricted Delaunay triangulation – see definition 1. We show that the algorithm terminates on a wide variety of input surfaces and allows to control both the size and the aspect ratio of the facets.
- taking advantage of recent theoretical results on the restricted Delaunay triangulation [11, 3, 6], we show how the algorithm can be turned into a quasi-optimal surface sampling and approximating program. Specifically, we show that it can generate good samples – see definition 3 – on smooth closed surfaces. From this result we deduce that the restricted Delaunay triangulation has the right topology type and approximates the original surface in terms of Hausdorff distance, normals and area.
- we provide experimental evidence that the algorithm works well in practice and is able to deal with boundaries. The practical results on piecewise smooth surfaces are encouraging and attest that the algorithm is also suitable for polyhedral surface remeshing.

## 2 Restricted Delaunay triangulation and point samples

In this section,  $S$  is a 2-manifold embedded in  $\mathbb{R}^3$ , and  $Y$  is a point sample of  $S$ . By  $\text{Del}(Y)$  we denote the 3-dimensional Delaunay triangulation of  $Y$ .

**Definition 1** *The Delaunay triangulation of  $Y$  restricted to  $S$ , noted  $\text{Del}_{|S}(Y)$ , is the sub-complex of  $\text{Del}(Y)$  that consists of the facets of  $\text{Del}(Y)$  whose dual Voronoi edges intersect  $S$ . For any facet  $f$  of  $\text{Del}_{|S}(Y)$ , we call surface Delaunay ball of  $f$  any empty ball circumscribed to  $f$  whose center lies on  $S$ .*

### Definition 2

- we call maximal ball any ball that is maximal (with respect to the inclusion) among the set of open balls included in  $\mathbb{R}^3 \setminus S$ .
- the skeleton of  $S$ , noted  $\sigma$ , is the topological closure of the union of the centers of all maximal balls.
- for a point  $x \in \mathbb{R}^3$ , we call distance to the skeleton at  $x$ , and write  $d_\sigma(x)$ , the Euclidean distance from  $x$  to the skeleton of  $S$ . According to lemma 1 of [3],  $d_\sigma$  is 1-Lipschitz.

**Lemma 1** (from proposition 13 of [5])

Let  $B$  be a ball that intersects  $S$  (resp. the boundary  $\partial S$  of  $S$ ). If the intersection is not a topological disc (resp. a topological arc), then  $B$  contains a point of the skeleton of  $S$  (resp.  $\partial S$ ).

**Definition 3** (from [3, 4])

Given a 1-Lipschitz function  $\phi : S \rightarrow \mathbb{R}$ ,  $Y$  is an  $\varepsilon$ -sample of  $S$  with respect to  $\phi$  if  $\forall x \in S$ ,  $|Y \cap B(x, \varepsilon \phi(x))| \geq 1$ . Most of the time  $\phi = d_\sigma$ , which will be assumed by default.

- If  $\phi$  is constant (say  $\phi = 1$ ), then  $Y$  is called a uniform  $\varepsilon$ -sample.

- If  $\forall x \in S$ ,  $1 \leq |Y \cap B(x, \varepsilon \phi(x))| \leq \kappa$ , then the sample is called an  $(\varepsilon, \kappa)$ -sample.

Erickson [12] has shown that  $\Omega \left( \frac{\mu(S)}{\varepsilon^2} \right)$ , with  $\mu(S) = \int_S \frac{dx}{d_\sigma^2(x)}$ , is a lower bound on the number of points of any  $\varepsilon$ -sample of  $S$ , with  $\varepsilon < \frac{1}{5}$ . If an  $\varepsilon$ -sample of  $S$  contains  $O \left( \frac{\mu(S)}{\varepsilon^2} \right)$  points, then it is said to be sparse.

Now we introduce two results on the restricted Delaunay triangulation that are proved in [6]. They will be used in sections 5 and 6.

**Theorem 1** Assume that  $S$  is smooth, compact, without boundaries, and that the distance to its skeleton  $\sigma$  has a lower bound  $d_\sigma^{\min} > 0$ . Assume also that  $\text{Del}_S(Y)$  has at least one facet on each connected component of  $S$ .

- if  $\forall f \in \text{Del}_S(Y)$  each surface Delaunay ball of  $f$  has a radius at most  $\frac{\varepsilon}{4}$ , where  $\varepsilon \leq 0.36 d_\sigma^{\min}$ , then the set of vertices of  $\text{Del}_S(Y)$  is a uniform  $\varepsilon$ -sample of  $S$

- if  $\forall f \in \text{Del}_S(Y)$  each surface Delaunay ball  $B(c_f, r_f)$  of  $f$  has a radius  $r_f$  not greater than  $\frac{\varepsilon}{6+5\varepsilon} d_\sigma(c_f)$ , where  $\varepsilon \leq 0.66$ , then the set of vertices of  $\text{Del}_S(Y)$  is an  $\varepsilon$ -sample of  $S$ .

**Theorem 2** Assume that  $S$  is smooth and compact, and that  $Y$  is an  $\varepsilon$ -sample of  $S$ , with  $\varepsilon \leq \frac{1}{2}$ . If  $S$  has some boundaries, then assume that  $Y$  contains a  $\mu$ -sample of  $\partial S$ , with  $\mu < \frac{1}{1+2\sqrt{2}}$ . Let  $K$  be a positive number and  $\psi : S \rightarrow \mathbb{R}$  a 1-Lipschitz function such that

$$\forall v \in Y, \text{dist}(v, Y \setminus \{v\}) \geq K \psi(v) \quad (1)$$

Then

$$|Y| \leq C \frac{\left(1 + K(\sqrt{2} - 1)\right)^2}{\pi(\sqrt{2} - 1)^2 K^2} \int_S \frac{dx}{\psi^2(x)}$$

where  $C = 10$  if  $S$  has some boundaries and  $C = \frac{4}{3}$  otherwise.

### 3 Chew's algorithm

The algorithm takes as input a pair  $(S, X)$ , where  $S$  is a compact surface and  $X$  is a set of points lying on  $S$ . If  $X$  has some points on the boundary  $\partial S$  of  $S$ , we call boundary edges the segments that join consecutive points of  $X$  on  $\partial S$ .

The algorithm uses a set of points  $\bar{X}$ , which is initialized to  $X$  and progressively enriched with new points, and maintains its restricted Delaunay triangulation  $\text{Del}_S(\bar{X})$  throughout the process. Procedure  $\text{insert}(p)$  adds point  $p$  to  $\bar{X}$  and updates  $\text{Del}_S(\bar{X})$ . If  $e$  is a boundary edge that is "encroached" (ie there exists a point of  $\bar{X}$  that lies inside its diametral ball),  $\text{midpoint}(e)$  returns an intersection point of the bisector of  $e$  and  $\partial S$ . When this point is inserted, the edges it forms with the vertices of  $e$  become boundary edges, whereas  $e$  is no longer a boundary edge. For a facet  $f$  of  $\text{Del}_S(\bar{X})$ ,  $\text{circumcenter}(f)$  returns the center of a surface Delaunay ball of  $f$ . The algorithm is templated by a criterion  $\rho$  on the facets of  $\text{Del}_S(\bar{X})$ .

## ALGORITHM

INITIALISATION

$\bar{X} = X$ ; compute  $\text{Del}_S(\bar{X})$

REPEAT

WHILE there remains any encroached  
boundary edge  $e$

$\text{insert}(\text{midpoint}(e))$

LET  $f$  be any facet of  $\text{Del}_S(\bar{X})$  that does not  
meet  $p$

LET  $p = \text{circumcenter}(f)$

IF  $p$  encroaches boundary edges  $s_1, \dots, s_k$ ,

THEN

FOR  $i = 1$  TO  $k$

$\text{insert}(\text{midpoint}(s_i))$

ELSE

$\text{insert}(p)$

UNTIL no boundary edge is encroached and  
all facets of  $\text{Del}_S(\bar{X})$  meet  $p$

At the end of the process the algorithm returns  $\bar{X}$  and  $\text{Del}_S(\bar{X})$ . Originally, Chew's algorithm did not compute the 3-dimensional Delaunay triangulation of the points. However, there are several advantages in using a 3-dimensional triangulation: it allows to handle topology changes, which is important especially during the first steps of the algorithm, and it provides a location data structure that allows to insert new points fast [10].

As for  $p$ , we shall use two measures: the aspect ratio and the size of the facets.

**Definition 4** (*some refinement criteria*)

Let  $f$  be a facet of  $\text{Del}_S(\bar{X})$ . We call  $\theta$  its smallest angle and  $B_f = B(c_f, r_f)$  its biggest surface Delaunay ball:

( $\rho_{\text{aspect ratio}}$ )  $f$  meets the criterion if  $\frac{1}{2\sin\theta} \leq B$ ,  
where  $B$  is a positive constant

( $\rho_{\text{size}}$ )  $f$  meets the criterion if  $r_f \leq g(c_f)$ ,  
where  $g: S \rightarrow \mathbb{R}$  has a lower  
bound  $h > 0$

An easy computation shows that for any triangle  $t$  with smallest angle  $\theta$ ,  $\frac{1}{2\sin\theta}$  is equal to the ratio between the radius of the circumcircle of  $t$  and the length of its smallest edge.

The algorithm can use one of the above criteria or it can combine them. For instance, one can first remove facets that are too big and then remove facets with a bad aspect ratio.

## 4 Termination of the algorithm

We prove that Chew's algorithm terminates after a finite number of steps. This result holds for surfaces without boundaries or with smooth or piecewise linear boundaries.

**Definition 5** Let  $v$  be a point inserted by the algorithm. We call insertion radius of  $v$  (noted  $r_v$ ) the distance from  $v$  to the "current" set of points  $\bar{X}$  at the time when  $v$  is inserted. By convention, the insertion radius of any vertex  $w$  of the input point sample  $X$  is  $\text{dist}(w, X \setminus \{w\})$ .

The proof of termination relies on the fact that the insertion radius remains greater than a constant during the whole process. It follows that the points inserted by the algorithm cannot get too close to one another, and thus cannot be infinitely many.

**Theorem 3** *Let  $S$  be a compact surface and  $X$  a point sample of  $S$ . The algorithm is applied to  $(S, X)$ :*

- *If  $S$  has no boundary, then the algorithm will terminate provided that  $B \geq 1$ .*
- *If  $S$  has piecewise linear boundaries such that all angles between consecutive boundary edges are greater than  $\pi/4$ , then the algorithm will terminate provided that  $B \geq \sqrt{2}$ .*
- *If  $S$  has smooth boundaries and if the initial set of points  $X$  contains a  $\mu$ -sample of  $\partial S$ , with  $\mu < 1/3$ , then the boundary edges make no angle less than  $2\pi/3$  and the algorithm will terminate provided that  $B \geq \frac{2\mu}{\sqrt{1-2\mu-3\mu^2-(1-3\mu)}} \sqrt{2}$ .*

**Proof** The proof of the first two statements is similar to Shewchuk's proof for the planar case [22] and is omitted here. As for the third statement, the proof differs slightly but keeps the same flavour. Consider a point  $v$  that is inserted by the algorithm. We distinguish three different cases:

- $v$  is the "circumcenter" of a facet  $f$ . By definition, the Delaunay ball  $\sigma_f$  of  $f$  that is centered at  $v$  is empty. Hence, the insertion radius  $r_v$  is equal to the radius of  $\sigma_f$ . If  $v$  is inserted because  $f$  does not meet  $\rho_{size}$ , then the radius of  $\sigma_f$  is greater than  $h$ . If  $v$  is inserted because  $f$  does not meet  $\rho_{aspect\ ratio}$ , then the radius of  $\sigma_f$  is not less than the radius of the circumcircle of  $f$ . Let  $p$  be the vertex of the smallest edge of  $f$  that has been inserted last. By definition, its insertion radius  $r_p$  is not greater than the length of the smallest edge of  $f$ . Since  $f$  does not meet the criterion ( $\rho_{aspect\ ratio}$ ), we have  $\frac{r_v}{r_p} \geq \frac{\text{radius of circumcircle}}{\text{length of smallest edge}} \geq B$ .
- $v$  is the "midpoint" of a boundary edge  $[a, b]$  that is encroached by a circumcenter  $p$ . We know that  $[a, b]$  is encroached only by  $p$  and that  $p$  will not be inserted. The insertion radius  $r_p$  of  $p$  is less than  $\|a - b\| \frac{\sqrt{2}}{2}$  since  $p$  lies in the diametral ball of  $[a, b]$ . So, according to lemma 5, the insertion radius  $r_v$  of  $v$  is such that

$$\begin{aligned} r_v &\geq \delta_v \geq \frac{\sqrt{1-2\mu-3\mu^2-(1-3\mu)} \|a-b\|}{2\mu} \\ &\geq \frac{\sqrt{1-2\mu-3\mu^2-(1-3\mu)}}{2\mu} \frac{1}{\sqrt{2}} r_p \end{aligned}$$

- $v$  is the "midpoint" of a boundary edge that is encroached by the vertex of an adjacent boundary edge. In fact, this situation cannot occur: indeed, according to lemma 4, all angles between boundary edges are greater than  $2\pi/3$ , since  $\mu < \frac{1}{3}$ .

The different cases are summarized in the flow graph of figure 1:

- If  $S$  has no boundary, then only loop (1) may occur. Hence, with  $B \geq 1$ , the insertion radius does not decrease when a badly shaped facet is split, whereas it remains greater than  $h$  when a badly sized facet is split. Thus during the whole process the insertion radius remains greater than  $d = \min(e, h)$ , where  $e$  is the minimal distance between any two vertices of the input set of points.

- If  $S$  has smooth boundaries, then taking  $B \geq \frac{2\mu}{\sqrt{1-2\mu-3\mu^2-(1-3\mu)}} \sqrt{2}$  makes the coefficients of loops (1) and (1) + (2) greater than 1, which implies that the insertion radius, throughout the process, remains greater than  $d = \min\left(e, \frac{\sqrt{1-2\mu-3\mu^2-(1-3\mu)}}{2\mu} \frac{h}{\sqrt{2}}\right)$ .

In both cases, every point  $v$  of  $\bar{X}$  remains at distance at least  $d$  from any other point of  $\bar{X}$ . It follows that the open balls of radius  $\frac{d}{2}$  centered at the points of  $\bar{X}$  are pairwise disjoint. Now consider the volume  $V = \{x \in \mathbb{R}^3 \mid \text{dist}(x, S) \leq \frac{d}{2}\}$ . This volume is clearly bounded since the surface is compact, and it contains  $\cup_{v \in \bar{X}} B_v$ , which implies that there can be only a finite number of pairwise disjoint balls.  $\square$

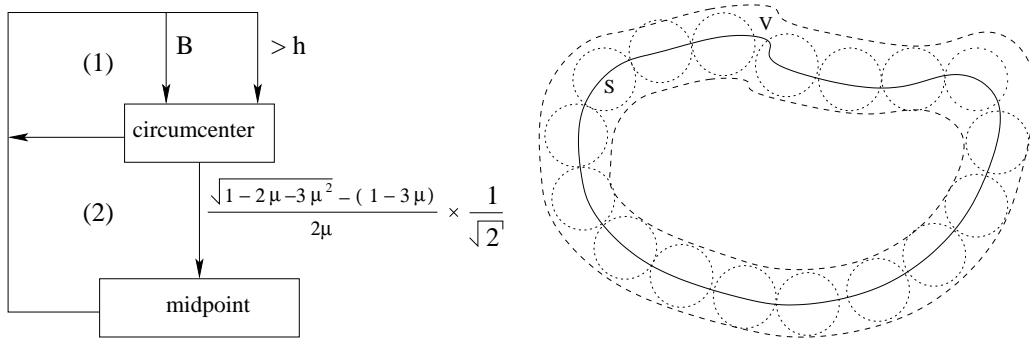


Figure 1: Flow graph and volume  $V$

Observe that theorem 3 asserts that, if  $S$  has no boundary, the algorithm generates meshes with no angle less than 30 degrees if one sets  $B = 1$ . If  $S$  has polygonal boundaries, no angle less than 20.7 degrees is created if one sets  $B = \sqrt{2}$ .

## 5 Approximating the surface

In this section,  $S$  denotes a smooth compact surface without boundaries such that, for any  $x \in S$ ,  $d_\sigma(x) \geq d_\sigma^{\min} > 0$ . Let  $X$  be a finite set of points on  $S$ . The algorithm is applied to  $(S, X)$  with the criterion  $(\rho_{size})$ , parameterized by a function  $g$  which is 1-Lipschitz. We call  $\bar{X}$  the point sample generated by the algorithm.

We shall show that the algorithm can produce sparse  $\varepsilon$ -samples. We first consider the general case, and afterwards the case of uniform samples, for which better bounds can be provided. Approximation results come out as corollaries.

### 5.1 Generating $\varepsilon$ -samples

To establish our results, we use theorem 1 which requires  $\text{Del}_{|S}(\bar{X})$  to be non-empty. The following lemma helps ensuring this condition.

**Lemma 2** *Assume that there exists a facet  $f_0$  of  $\text{Del}_{|S}(X)$  that has a surface Delaunay ball  $B_{f_0} = B(c_{f_0}, r_{f_0})$  such that  $r_{f_0} \leq \frac{1}{3} g(c_{f_0})$ . Then  $f_0 \in \text{Del}_{|S}(\bar{X})$ .*

**Proof** Assume that, at the end of the algorithm,  $f_0 \notin \text{Del}_{|S}(\bar{X})$ . This implies that there exists a step at which the algorithm inserted a point  $v$  inside  $B_{f_0}$ . According to the size criterion,  $v$  is the center of a Delaunay ball  $B_f$  of a certain facet  $f$ , such that the radius  $r_f$  of  $B_f$  is greater than  $g(v)$ .

Since  $v$  lies inside  $B_{f_0}$ , we have  $\|v - c_{f_0}\| < \frac{1}{3} g(c_{f_0})$ . And, since  $g$  is 1-Lipschitz,

$$g(v) \geq g(c_{f_0}) - \|v - c_{f_0}\| > \left(1 - \frac{1}{3}\right) g(c_{f_0})$$

Let  $a$  be one of the vertices of  $f_0$ . Since  $a$  is in  $B_{f_0}$ , we have

$$\|a - v\| \leq 2 r_{f_0} \leq \frac{2}{3} g(c_{f_0}) < g(v) < r_f$$

which contradicts the fact that  $B_f$  is a Delaunay ball.  $\square$

**Definition 6**  $f_0$ , defined as in the above lemma, is called **seed-facet** – see figure 2. Note that, despite the fact that  $f_0$  has one small surface Delaunay ball, it may have also big ones that will eventually be deleted by the algorithm. However, lemma 2 claims that the small one will remain.

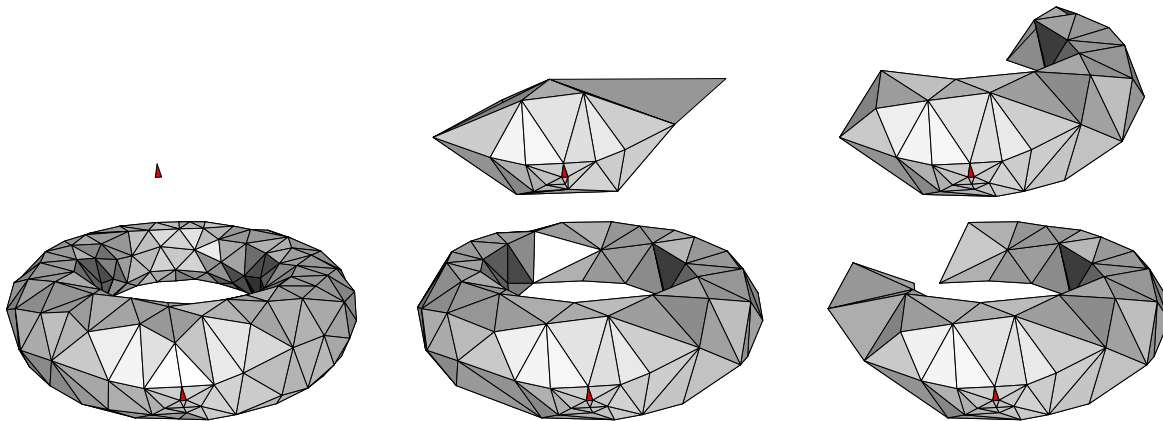


Figure 2: Meshing process on the torus of equation  $(1.5 - \sqrt{x^2 + y^2})^2 + z^2 - 0.25 = 0$ , with a uniform size criterion of  $10^{-1}$  and three starting points: the seed-facet remains in the restricted Delaunay triangulation throughout the process.

From lemma 2 and theorem 1 we deduce that the algorithm can build  $\varepsilon$ -samples:

**Theorem 4** Let  $\varepsilon$  be a positive constant such that  $\varepsilon \leq 0.66$ . We set  $g \leq \frac{\varepsilon}{6+5\varepsilon} d_\sigma$ . Assume that  $\text{Del}_{|S}(X)$  has a seed-facet on each connected component of  $S$ . Then the vertices of  $\text{Del}_{|S}(\bar{X})$  form an  $\varepsilon$ -sample of  $S$ .

**Proof** Lemma 2 ensures that  $\text{Del}_{|S}(\bar{X})$  has at least one facet on each connected component of  $S$ . In addition, the size criterion ensures that every surface Delaunay ball  $B(c_f, r_f)$  of any facet  $f$  of  $\text{Del}_{|S}(\bar{X})$  is such that  $r_f \leq g(c_f) \leq \frac{\varepsilon}{6+5\varepsilon} d_\sigma(c_f)$ . So, the assumptions of theorem 1 are verified, which gives the result.  $\square$

**Remark** The vertices of  $\text{Del}_{|S}(\bar{X})$  belong to  $\bar{X}$  (hence theorem 4 implies that  $\bar{X}$  is an  $\varepsilon$ -sample of  $S$ ), but the converse is not necessarily true.

## 5.2 Approximation results

In this section, we give approximation results that are consequences of the fact that the algorithm can build  $\varepsilon$ -samples.

### Topological guarantees

Theorem 2 of [3] states that the restricted Delaunay triangulation of an  $\varepsilon$ -sample of  $S$ , with  $\varepsilon < 0.1$ , is homeomorphic to  $S$ . From this result and theorem 4 we deduce the following corollary:

**Corollary 1** Under the assumptions of theorem 4, with  $\varepsilon < 0.1$ ,  $S$  and  $\text{Del}_{|S}(\bar{X})$  are homeomorphic.

## Hausdorff distance

The fact that  $\bar{X}$  belongs to  $S$  is useful for bounding the Hausdorff distance between  $S$  and  $\text{Del}_{|S}(\bar{X})$ . The following result says that, once the surface  $S$  is given, the Hausdorff distance between  $S$  and  $\text{Del}_{|S}(\bar{X})$  is  $O(\varepsilon)$ :

**Corollary 2** *Under the assumptions of theorem 4, with  $\varepsilon \leq 0.66$ , the Hausdorff distance between  $S$  and  $\text{Del}_{|S}(\bar{X})$  is bounded by  $\varepsilon d_\sigma^{\max}$ , where  $d_\sigma^{\max} = \max \{d_\sigma(x), x \in S\}$ .*

**Proof** On the one hand, we use the criterion ( $\rho_{size}$ ) with  $g \leq \frac{\varepsilon}{6+5\varepsilon} d_\sigma \leq \varepsilon d_\sigma$ , which implies that every facet of  $\text{Del}_{|S}(\bar{X})$  has a radius less than  $\varepsilon d_\sigma^{\max}$ . It follows that every point of  $\text{Del}_{|S}(\bar{X})$  is at distance less than  $\varepsilon d_\sigma^{\max}$  from  $\bar{X} \subseteq S$ .

On the other hand, theorem 4 says that the vertices of  $\text{Del}_{|S}(\bar{X})$  form an  $\varepsilon$ -sample of  $S$ . Thus every point of  $S$  is at distance less than  $\varepsilon d_\sigma^{\max}$  from those vertices, and hence from the restricted Delaunay triangulation.  $\square$

## Normals approximation

Lemma 7<sub>(b)</sub> of [3] bounds the angle between the normal to any facet  $f$  of  $\text{Del}_{|S}(\bar{X})$  and the normal to the surface at each of the vertices of  $f$ , when  $\bar{X}$  is an  $\varepsilon$ -sample of  $S$ . From this result and theorem 4 we deduce the following:

**Corollary 3** *Under the assumptions of theorem 4, with  $\varepsilon < \frac{1}{7}$ , the angle between the normal to any facet  $f$  of  $\text{Del}_{|S}(\bar{X})$  and the normal to  $S$  at any of the vertices of  $f$  is less than  $\frac{2\varepsilon}{1-7\varepsilon} + \arcsin \frac{\sqrt{3}\varepsilon}{1-\varepsilon}$ .*

## Area approximation

If  $\bar{X}$  is an  $\varepsilon$ -sample of  $S$ , then the area of  $\text{Del}_{|S}(\bar{X})$  approximates the area of  $S$  – see [20]. From this result and theorem 4 we deduce the following:

**Corollary 4** *Under the assumptions of theorem 4, with  $\varepsilon \leq 0.66$ , there exist two constants  $C_1$  and  $C_2$  depending on  $\varepsilon$ , such that  $C_1 \text{Area}(S) \leq \text{Area}(\text{Del}_{|S}(\bar{X})) \leq C_2 \text{Area}(S)$ , and  $\lim_{\varepsilon \rightarrow 0} C_1(\varepsilon) = \lim_{\varepsilon \rightarrow 0} C_2(\varepsilon) = 1$ .*

## 5.3 Sparse $\varepsilon$ -samples

Provided that  $X$  contains few points, the algorithm actually produces sparse  $\varepsilon$ -samples. For simplicity, we assume that  $X$  contains exactly three points per connected component of  $S$ . This is no real loss of generality and the following result holds for any set  $X$  of constant size.

**Theorem 5** *Let  $\varepsilon$  be a positive constant such that  $\varepsilon \leq \frac{\sqrt{57}-7}{4} \approx 0.14$ . We set  $g = \frac{\varepsilon}{6+5\varepsilon} d_\sigma$ . Assume that  $X$  has exactly 3 points per connected component of  $S$ , and that  $\text{Del}_{|S}(X)$  has a seed-facet on each connected component of  $S$ . Then  $\bar{X}$  is a sparse  $\varepsilon$ -sample of  $S$ .*

**Proof** Since  $\varepsilon \leq \frac{\sqrt{57}-7}{4} \leq 0.66$  and  $\text{Del}_{|S}(X)$  has a seed-facet on each connected component of  $S$ , theorem 4 implies that  $\bar{X}$  is an  $\varepsilon$ -sample of  $S$ .

To bound the cardinality of  $\bar{X}$ , we shall use theorem 2 with  $Y = \bar{X} \setminus X$ . We first show that  $\bar{X} \setminus X$  is a  $\frac{1}{2}$ -sample of  $S$ . Let  $S_i$  be a connected component of  $S$ . We have  $\varepsilon < 1$ , thus at any point  $x \in S_i$ ,  $B(x, \varepsilon d_\sigma(x)) \cap S$  is a topological disc. Therefore,  $B(x, \varepsilon d_\sigma(x))$  intersects  $S_i$  only. This means that, since  $\bar{X}$  is an  $\varepsilon$ -sample of

$S$ , we have  $\forall x \in S_i, |B(x, \varepsilon d_\sigma(x)) \cap S_i \cap \bar{X}| \geq 1$ , ie  $\bar{X} \cap S_i$  is an  $\varepsilon$ -sample of  $S_i$  with respect to  $d_\sigma$ . Let  $f_i$  be the seed-facet associated with  $S_i$ . Since  $g = \frac{\varepsilon}{6+5\varepsilon} d_\sigma < 0.17 d_\sigma$ , lemma 6 ensures that every edge of  $f_i$  is incident to another facet of  $\text{Del}_S(\bar{X})$ . Moreover, since  $g < d_\sigma$ , every facet of  $\text{Del}_S(\bar{X})$  has its three vertices in the same connected component of  $S$ . In particular, all the facets of  $\text{Del}_S(\bar{X})$  that are incident to  $f_i$  have their vertices in  $S_i$ . So, the assumptions of lemma 7 are verified, with  $\Sigma = S_i$  and  $\phi = d_\sigma$ , hence  $\bar{X} \cap S_i$  minus the set of vertices of  $f_i$  is a  $\frac{(3+\varepsilon)\varepsilon}{1-\varepsilon}$ -sample of  $S_i$  with respect to  $d_\sigma$ . By assumption, the set of vertices of  $f_i$  is exactly  $X \cap S_i$ , thus  $(\bar{X} \cap S_i) \setminus (X \cap S_i)$  is a  $\frac{(3+\varepsilon)\varepsilon}{1-\varepsilon}$ -sample of  $S_i$  with respect to  $d_\sigma$ . Since this is true for every connected component of  $S$ , we conclude that  $\bar{X} \setminus X$  is a  $\frac{(3+\varepsilon)\varepsilon}{1-\varepsilon}$ -sample of  $S$ . Here we have  $\varepsilon \leq \frac{\sqrt{57}-7}{4}$ , thus  $\frac{(3+\varepsilon)\varepsilon}{1-\varepsilon} \leq \frac{1}{2}$ .

Now, let  $v$  be a point of  $\bar{X} \setminus X$ , ie a point that has been inserted by the algorithm. Let  $w$  be the point of  $\bar{X}$  that is closest to  $v$ . We distinguish two cases: 1.  $w \in X$  or has been inserted before  $v$ , 2.  $w$  has been inserted after  $v$ . In the former case, we have, according to the size criterion,

$$\|v - w\| > \frac{\varepsilon}{6+5\varepsilon} d_\sigma(v)$$

In the latter case, we have, for the same reason,

$$\|v - w\| > \frac{\varepsilon}{6+5\varepsilon} d_\sigma(w) \geq \frac{\varepsilon}{6+5\varepsilon} (d_\sigma(v) - \|v - w\|)$$

which gives

$$\|v - w\| > \frac{\varepsilon}{6(1+\varepsilon)} d_\sigma(v)$$

In both cases, we have  $\text{dist}(v, (\bar{X} \setminus X) \setminus \{v\}) \geq \text{dist}(v, \bar{X} \setminus \{v\}) = \|v - w\| > \frac{\varepsilon}{6(1+\varepsilon)} d_\sigma(v)$ . Since  $\bar{X} \setminus X$  is a  $\frac{(3+\varepsilon)\varepsilon}{1-\varepsilon}$ -sample of  $S$ , with  $\frac{(3+\varepsilon)\varepsilon}{1-\varepsilon} \leq \frac{1}{2}$ , theorem 2 (with  $Y = \bar{X} \setminus X$ ,  $\psi = d_\sigma$  and  $K = \frac{\varepsilon}{6(1+\varepsilon)}$ ) says that

$$|\bar{X} \setminus X| \leq \frac{4 \left(6 + (\sqrt{2} + 5)\varepsilon\right)^2}{3\pi(\sqrt{2} - 1)^2} \frac{\int_S \frac{dx}{d_\sigma^2(x)}}{\varepsilon^2}$$

Now, by assumption,  $|X| = 3k$ , where  $k$  is the number of connected components of  $S$ . Thus  $|\bar{X}| = 3k + |\bar{X} \setminus X|$ . Note that for any connected component  $S_i$  of  $S$ , the distance to the skeleton  $\sigma_i$  of  $S_i$  (considered independently from the other connected components of  $S$ ) is greater than  $\frac{1}{2} d_\sigma$ . Thus,  $\int_{S_i} \frac{dx}{d_\sigma^2(x)} \geq \frac{1}{4} \int_{S_i} \frac{dx}{d_{\sigma_i}^2(x)}$ , which is greater than  $\pi$  according to lemma 8. Hence  $\int_S \frac{dx}{d_\sigma^2(x)} \geq \pi k$ , which gives

$$|\bar{X}| \leq \left( \frac{3\varepsilon^2}{\pi} + \frac{4 \left(6 + (\sqrt{2} + 5)\varepsilon\right)^2}{3\pi(\sqrt{2} - 1)^2} \right) \frac{\int_S \frac{dx}{d_\sigma^2(x)}}{\varepsilon^2}$$

and, since  $\varepsilon \leq \frac{\sqrt{57}-7}{4}$ ,

$$|\bar{X}| \leq \left( \frac{3 \left(\sqrt{57} - 7\right)^2}{16\pi} + \frac{\left(24 + (\sqrt{2} + 5)(\sqrt{57} - 7)\right)^2}{12\pi(\sqrt{2} - 1)^2} \right) \times \frac{\int_S \frac{dx}{d_\sigma^2(x)}}{\varepsilon^2} < 117.17 \times \frac{\int_S \frac{dx}{d_\sigma^2(x)}}{\varepsilon^2}$$

□

## Remarks

Since the vertices of  $\text{Del}_S(\bar{X})$  belong to  $\bar{X}$ , the above result and theorem 4 imply that they also form a sparse  $\varepsilon$ -sample of  $S$ .

The lower bound given by Erickson [12] is  $\frac{9}{50\pi} \frac{\mu(S)}{\varepsilon^2}$ , thus Chew's algorithm is a 2045-approximation algorithm for the problem of  $\varepsilon$ -sampling! Note that, when  $\varepsilon$  tends to zero, our upper bound is equivalent to  $\frac{48}{\pi(\sqrt{2}-1)^2} \frac{\mu(S)}{\varepsilon^2}$ , which is about 1500 times the lower bound of Erickson.

## 5.4 Generating uniform samples

If one takes the function  $g$  of the size criterion to be constant (note that it is still 1-Lipschitz), then the algorithm will generate uniform samples. In fact, if  $\bar{X}$  is an  $\varepsilon$ -sample, then it is a uniform  $(\varepsilon d_\sigma^{\max})$ -sample, where  $d_\sigma^{\max} = \max \{d_\sigma(x), x \in S\}$ . The results of the previous subsections therefore hold. However, better bounds can be obtained, as shown below.

**Theorem 6** *We set  $g = h$ , where  $h$  is a positive constant less than  $0.09 d_\sigma^{\min}$ . Assume that  $X$  has exactly three points per connected component of  $S$ , and that  $\text{Del}_S(\bar{X})$  has a seed-facet on each connected component of  $S$ . Then  $\bar{X}$  is a uniform  $(4h, 515)$ -sample of  $S$ .*

**Proof** Lemma 2 ensures that  $\text{Del}_S(\bar{X})$  has at least one facet on each connected component of  $S$ . Thus, since  $4h \leq 0.36 d_\sigma^{\min}$ , we can use theorem 1 which says that the vertices of  $\text{Del}_S(\bar{X})$  form a uniform  $4h$ -sample of  $S$ . It follows that  $\bar{X}$  is also a uniform  $4h$ -sample of  $S$ .

Now, let  $v$  be a point of  $\bar{X} \setminus X$ , i.e. a point that has been inserted by the algorithm. Let  $w$  be any point of  $(\bar{X} \setminus X) \setminus \{v\}$ . If  $w$  has been inserted before  $v$ , then according to the size criterion we have  $\|v - w\| > h$ . If  $w$  has been inserted after  $v$ , then the size criterion also says that  $\|v - w\| > h$ . Thus, the points of  $\bar{X} \setminus X$  are centers of pairwise disjoint balls of radius  $\frac{h}{2}$ . Hence, for every point  $x \in S$ , the number of points of  $\bar{X} \setminus X$  that lie inside  $B(x, 4h)$  is less than

$$\frac{\frac{4}{3} \pi (4h)^3}{\frac{4}{3} \pi \left(\frac{h}{2}\right)^3} = 512$$

Since  $4h < d_\sigma^{\min}$ , at each point  $x \in S$  the ball  $B(x, 4h)$  intersects only the connected component of  $S$  where  $x$  lies. Thus, since  $X$  has exactly three points per connected component, we have  $|B(x, 4h) \cap X| \leq 3$ . Hence the number of points of  $\bar{X}$  that lie inside  $B(x, 4h)$  is less than  $512 + 3 = 515$ .  $\square$

**Remark** The fact that  $\bar{X}$  is a uniform  $(\varepsilon, \kappa)$ -sample implies that, once the surface is given, the size of  $\bar{X}$  is  $O\left(\frac{1}{\varepsilon^2}\right)$ , which is optimal for uniform  $\varepsilon$ -samples.

## 6 Bounding the aspect ratio

Once an approximation of the surface has been obtained (or is given), the algorithm can be used to remove the skinny facets: this can be done with the help of the criterion ( $\rho_{\text{aspect ratio}}$ ). Theorem 3 gives bounds on the angles of the facets of the resulting triangulated surface. The following result provides a worst-case optimal upper bound on the size of the output with respect to the size of the input. It roughly shows that we can bound the aspect ratio of the triangles without significantly increasing the number of vertices.

**Definition 7** *Let  $S$  be a surface and  $X$  a set of points sampled from  $S$ . Consider the graph  $G$  made of the vertices of  $X$  and of the boundary edges of  $S$ . The local feature size at  $x$ , noted  $\text{lfs}_X(x)$ , is defined as the radius of the smallest ball centered at  $x$  that intersects two nonincident vertices or edges of  $G$ .  $\text{lfs}_X$  is 1-Lipschitz [21].*

**Theorem 7** Let  $S$  be a smooth compact surface and  $X$  an  $\varepsilon$ -sample of  $S$ , with  $\varepsilon \leq \frac{1}{2}$ . If  $S$  has some boundaries, assume that  $X$  contains a  $\mu$ -sample of  $\partial S$ , with  $\mu < \frac{1}{2(1+\sqrt{2})}$ . If one runs the algorithm with the criterion ( $\rho_{aspect\ ratio}$ ) only, where  $B > \frac{2\mu}{\sqrt{1-2\mu-3\mu^2-(1-3\mu)}}\sqrt{2}$ , then the final number of points of  $\bar{X}$  is at most

$$C \cdot \int_S \frac{dx}{lfs_{\bar{X}}^2(x)}$$

where  $C$  is a constant that depends only on  $B$  and  $\mu$ .

**Proof** This result is a simple application of theorem 2. However, we have to make sure that equation (1) is verified. As in the planar case [21, 22], one can start from the relations that we established in the proof of theorem 3 and show that there exists a constant  $D_S \geq 1$  such that for every point  $v \in \bar{X}$ ,  $\frac{lfs_X(v)}{\text{dist}(v, \bar{X} \setminus \{v\})} \leq D_S + 1$ .

Hence, (1) holds with  $Y = \bar{X}$ ,  $\psi = lfs_X$  and  $K = \frac{1}{D_S+1}$ . We can then apply theorem 2 which gives the result.  $\square$

**Remark** Since the algorithm is output sensitive, it is important that the upper bound given here be relevant. In fact it is optimal in the worst case: indeed, if  $S$  is a planar surface then the problem becomes 2-dimensional, and according to Mitchell [19] any solution requires  $\Omega\left(\int_S \frac{dx}{lfs_X^2(x)}\right)$  points.

## 7 Experimental results – discussion

### Implementation

The algorithm has been implemented using the  $C^{++}$  library CGAL, which allowed us to derive the restricted Delaunay triangulation from the 3-dimensional Delaunay triangulation. Given a surface  $S$  and a point sample  $\bar{X}$ ,  $\text{Del}_S(\bar{X})$  is templated by the type of  $S$  – polyhedron, parametric or implicit surface etc – and is embedded in  $\text{Del}(\bar{X})$ . This requires a few additional features, e.g. special flags on the facets whose dual edges intersect  $S$ .

An advantage of the algorithm is that, except for the *in\_sphere()* predicate of the 3-dimensional Delaunay triangulation, the only predicate to implement is *does\_segment\_intersect\_surface()*, which tells whether a segment intersects the surface or not. Of course, there is also the corresponding constructor *intersect\_segment\_with\_surface()*, but its implementation keeps the same flavor. The predicate must be adapted to the type of the input surface. For instance, on an implicit surface given by the equation  $P(x, y, z) = 0$ , where  $P$  is a polynomial, one can use either an algebraic technique or a numerical technique. The former reduces to solve a univariate equation of degree  $\deg(P)$ , whereas the latter can be implemented as a simple binary search that uses the fact that if the signs of  $P$  at both endpoints are different then the segment intersects the surface. Although not exact and with a time complexity that depends on the precision of the search, the numerical approach is useful in practice since it can be extended to surfaces that are not algebraic or semi-algebraic.

Our theoretical results require to know some estimate of  $d_\sigma$ . If the algorithm is used with a uniform size criterion, we only need a lower bound  $d_\sigma^{\min}$ , which is available in many applications. If the algorithm is used with a local size criterion, we need an estimate of  $d_\sigma$  at all inserted points. One can approximate  $d_\sigma(x)$  by the distance from  $x$  to the set of poles [3] of the Voronoi diagram of  $\bar{X}$ . Although we do not have theoretical guarantees then, good results have been observed in practice – see figure 3 (center).

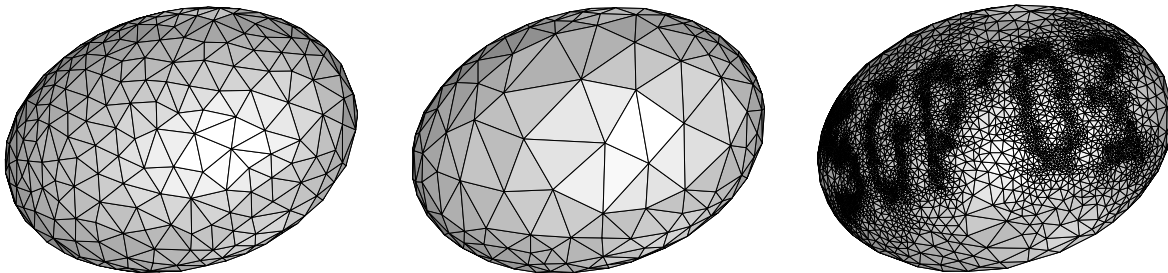


Figure 3: Various size criteria: uniform (left), curvature-adapted (center), customized (right).

### Timing and output complexity

Figure 4 shows the evolution of the output size and computation time (with a processor at 400 Mhz) with respect to the bound  $h$  of the size criterion, on the sphere of equation  $x^2 + y^2 + z^2 - 1 = 0$ . It turns out that the size of the output is  $O\left(\frac{1}{h^2}\right)$ , as predicted by theorems 5 and 6.

The algorithm is clearly output-sensitive. At each step it inserts a point in the 3-dimensional Delaunay triangulation. To this end, it deletes the facets that are in conflict with the point that is being inserted, and then triangulates the hole. For every new facet, it checks whether the dual Voronoi edge intersects the surface. Thus the behaviour of the algorithm is that of the incremental Delaunay triangulation, except that no point location is needed since only “circumcenters” of known facets or “midpoints” of known edges are inserted. It has been shown recently [4] that the size of the 3-dimensional Delaunay triangulation of an  $(\epsilon, \kappa)$ -sample of  $n$  points lying on a generic smooth surface is  $O(n \log n)$ . The worst-case time complexity of one step of the algorithm is thus  $O(\phi n \log n)$ , where  $\phi$  is the time complexity of the predicate *does\_segment\_intersect\_surface()* and  $n$  is the size of the current point sample. Note that  $\phi$  depends only on the surface and on the precision of the binary search, thus it can be considered as a constant here. This yields an overall worst-case time complexity of  $O(N^2 \log N)$ , where  $N$  is the size of the output. Assuming that the points are inserted in random order, the expected running time reduces to  $O(N \log N)$  since no point location is needed. This bound is usually observed in practice – see figure 4.

### About seed-facets

Figure 2 shows that seed-facets are preserved throughout the meshing process. The drawback of seed-facets is that, since they are smaller than the size criterion (at least three times as small), they force the algorithm to refine more in their vicinity than on the rest of the surface. This problem can be avoided by using no seed-facet and choosing a few random points to start the process. In that case there is no guarantee that the final restricted Delaunay triangulation will be non-empty. However, it is verified most of the time in practice. For instance, experiments have shown that, with the torus of figure 2 and exactly 3 initial random points, one has a 20% chance that the meshing process succeeds. If one chooses random points that have a smaller diameter, then the chance of success grows up dramatically (92% with a diameter of 0.5 which is still far above the size criterion). In addition, if one chooses a bigger initial set of random points, then the chance of success also grows up dramatically (40% with 4 points, 78% with 5 points, and more than 94% with 6 points). In conclusion, it is usually unnecessary to use seed-facets in practice. For instance, the results shown in figures 3, 5, 7, 6, 8, 9 and 10 were obtained without using any seed-facet. The initial point sets had various sizes, ranging from 3 points to a dozen of points.

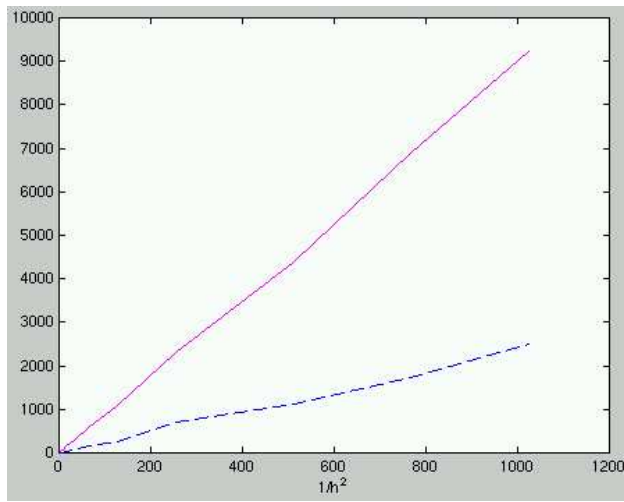


Figure 4: Output size (solid line) and time complexity (dashed line) versus  $\frac{1}{h^2}$ .

### Meshing smooth surfaces

Figure 5 shows some implicit surfaces that have been meshed by the algorithm, using as size criterion a linear function of  $d_\sigma$ . On the left is the “chair” of equation  $(x^2 + y^2 + z^2 - 23.75)^2 - 0.8((z - 5)^2 - 2x^2)((z + 5)^2 - 2y^2) = 0$ : degree 4 and genus 3. On the right is the “tanglecube” of equation  $x^4 - 5x^2 + y^4 - 5y^2 + z^4 - 5z^2 + 10 = 0$ : degree 4 and genus 5. Since both surfaces are closed and smooth, corollary 1 ensures that with a small enough size criterion the algorithm produces triangulated surfaces with the right topology type. This is observed here, even with a size criterion ( $g = 10^{-1}d_\sigma$ ) that is far above the theoretical bound. Figure 7 shows Barth’s decic surface (up) and Sheffer’s surface (down). The former has degree 10 and at least 40 singular points ! One can notice that these points have not been identified – see the zoom up right, so that the topology could not be captured. The result is a manifold except near the singularities, where  $d_\sigma$  tends to zero. The latter is periodic because its function is a trigonometric polynomial. Since it is not compact, we have only considered the portion of the surface that lies inside a ball.  $d_\sigma$  does not vanish on this surface and, as can be expected, the topology is preserved. However the result is not satisfactory near the boundaries, which are jagged because they were not set as “boundary edges”. Figure 6 shows some results on complex surfaces obtained from simple implicit primitives by applying boolean operations and offsets. The complex surfaces are meshed directly, without meshing first the primitives and then computing the boolean operations or the offsets on the triangulated primitives. The example in the middle is the solvent excluded surface of a molecule of alanin, with a probe of radius 20pm: this surface is a combination of spherical and toric patches – see the zoom on the left. The example on the right consists of two letters that were built as unions of cylinders.

### Dealing with boundaries and singularities

In the litterature, the usual method that is used to handle boundaries and singularities is to sample them before sampling the rest of the surface [2]. An advantage of Chew’s algorithm is that it allows to handle constrained boundaries and singularities at the same time as the rest of the surface. But how can one constrain a curve ? A way is to place a few sample points on it and constrain the corresponding segments. These segments become then “boundary edges” and are treated as such by the algorithm. When one of the segments has to be split, its bisector must be intersected with the curve, which is feasible if the curve

is piecewise linear or if we have its equation. In particular, boundaries of polyhedra are piecewise linear, whereas one can compute the equations of the boundaries and singularities of algebraic or semi-algebraic surfaces.

Constraining boundaries and singularities prevents their edges from being flipped, thus it greatly helps the algorithm manage them correctly. Figure 8 shows that constrained boundaries are preserved. On the left lies the end of a tubular surface remeshed by the algorithm (the original boundary is colored in blue). On the right, the implicit surface of equation  $z = \sin x \sin y$ , on the domain  $[-\pi, \pi] \times [-\pi, \pi]$ . Figure 9 shows the result of the algorithm on Steiner’s Roman surface, which is one of the three possible surfaces obtained by sewing a Moebius strip to the edge of a disk. This surface has one triple point, three singular lines and six pinch points. The singular lines, once constrained, were preserved by the algorithm, except near the pinch points.

Boundaries and singularities play different roles in the sampling theory. Indeed, by definition,  $d_\sigma$  tends to zero near a singularity, whereas it does not near a boundary. Thus it should be possible to extend our theoretical results to smooth surfaces with boundaries, whereas the sampling theory we currently use clearly fails in the vicinity of singularities. Practicle experiments corroborate this observation, since the result of the algorithm is always a manifold near boundaries, whereas it is not systematically near singularities.

### **The case of polyhedra.**

Theoretically, every edge of a polyhedron is problematic since it is singular. But in practice, it turns out that the results are manifold everywhere except near the sharp edges. A simple post-process that detects the edges with more than two incident facets and deletes the guilty facets often suffices to get a manifold surface. Note that constraining the sharp edges greatly helps the algorithm avoid non-manifold results. An example is shown in figure 10: the octopus was designed at first by an artist, using a quad-dominant mesh. We show the output of the algorithm, with a very thin size criterion adapted to  $d_\sigma$ , and a dozen of random points to start with. One can notice that the final point density is bigger near the edges of the initial mesh – see figure 10 (up right), and that all the details have been remarkably captured: see for instance the eyes – figure 10 (down right) – which are separate discs floating in the air.

## **8 Conclusion – future work**

We have revisited a greedy meshing algorithm. This algorithm can be applied to various types of surfaces and is quite simple. It is based on the 3-dimensional Delaunay triangulation and requires only few and simple additional predicates. We have given some theoretical guarantees. The algorithm can produce various kinds of samples and construct good approximations with respect to several criteria: topology, Hausdorff distance, normals, area.

We have implemented the algorithm and presented experimental results that corroborate (and sometimes are better than) the theory.

Currently, the theoretical results are limited to closed smooth surfaces, but it should be possible to extend them to smooth surfaces with boundaries as the experimental results suggest.

Handling the singularities is a more difficult issue that should require the use of a more general theory of surface sampling. However, the algorithm appears to be extremely robust even in the presence of singularities.

## Acknowledgments

The authors would like to thank David Cohen-Steiner and Marc Pouget for fruitful discussions, as well as Pierre Alliez for helpful remarks on the introductory and bibliographical sections of the paper.

## Appendix: Technical lemmata

### Results used to prove the termination of the algorithm

The following two lemmata come from [6]:

**Lemma 3** *Let  $C$  be a curve in  $\mathbb{R}^3$ . We call  $d_\zeta$  the distance to its skeleton  $\zeta$ . Let  $Y$  be a  $\mu$ -sample of  $C$ , with  $\mu < 1/2$ . Let  $a$  and  $b$  be two points of  $Y$  that are consecutive on  $C$ . Then*

$$\|a - b\| \leq \frac{2\mu}{1-\mu} d_\zeta(a)$$

**Lemma 4** *Let  $C$  be a curve in  $\mathbb{R}^3$ , and let  $Y$  be a  $\mu$ -sample of  $C$ , with  $\mu < 1/2$ . Let  $b$ ,  $a$  and  $c$  be three points of  $Y$  that are consecutive on  $C$ . Then*

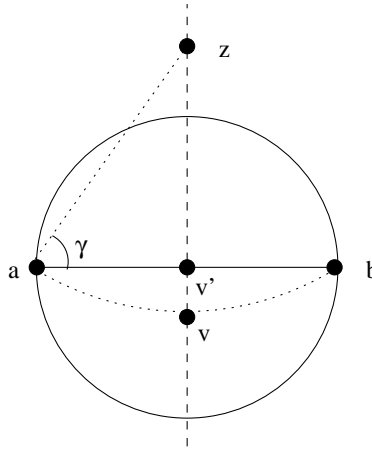
$$\widehat{bac} \geq 2 \arccos \frac{\mu}{1-\mu}$$

**Lemma 5** *Let  $S$  be a 2-manifold that has a smooth boundary. Let  $\tilde{X}$  be a finite set of points on  $S$  that contains a  $\mu$ -sample  $\tilde{X}$  of  $\partial S$ , with  $\mu < 1/3$ . Let  $a$  and  $b$  be two points of  $\tilde{X}$  that are consecutive on  $\partial S$ . If the boundary edge  $[a, b]$  is split by inserting point  $v \in \partial S$ , then*

$$\delta_v \geq \frac{\sqrt{1-2\mu-3\mu^2} - (1-3\mu)}{2\mu} \frac{\|a-b\|}{2}$$

where  $\delta_v$  is the distance from  $v$  to the diametral sphere of  $[a, b]$ .

**Proof** The point  $v$  which is inserted is at the intersection between  $\partial S$  and the bisector of  $[a, b]$ .



Let  $\zeta$  be the skeleton of  $\partial S$  and let  $z$  be any point of the bisector line of  $[a, b]$  in plane  $\Pi = (a, b, v)$ . If  $\gamma = \widehat{baz}$ , we have

$$\|z - a\| = \|z - b\| = \frac{\|a - b\|}{2 \cos \gamma}$$

And, according to lemma 3,

$$\|a - b\| \leq \frac{2\mu}{1-\mu} d_\zeta(a)$$

since  $a$  and  $b$  are consecutive points of  $\tilde{X}$  on  $\partial S$ .

Thus

$$\|z - a\| = \|z - b\| \leq \frac{\mu}{(1-\mu)\cos\gamma} d_\zeta(a)$$

which gives, since  $d_\zeta$  is 1-Lipschitz,

$$\begin{aligned} d_\zeta(z) &\geq d_\zeta(a) - \|z - a\| \\ &\geq \left( \frac{(1-\mu)\cos\gamma}{\mu} - 1 \right) \|z - a\| \end{aligned}$$

Now take point  $z$  so that  $\cos\gamma = \frac{2\mu}{1-\mu}$  and  $z$  is on the side of  $(a, b)$  that does not contain  $v$ .  $\gamma$  is well-defined as far as  $\mu \leq 1/3$ . For this particular value of  $\gamma$  we have

$$d_\zeta(z) \geq \|z - a\|$$

Thus point  $z$  is at the center of an open ball of radius  $\|z - a\|$  which does not intersect  $\zeta$ . According to lemma 1, the intersection between this ball and  $\partial S$  is a topological arc. And since points  $a$  and  $b$  are inside the ball, all points of  $\partial S$  between  $a$  and  $b$ , and in particular  $v$ , are also inside the ball. Hence the distance from  $v$  to the diametral sphere of  $[a, b]$  is

$$\begin{aligned} \delta_v &= \frac{\|a-b\|}{2} - \|v - v'\| \\ &\geq \frac{\|a-b\|}{2} - (\|z - a\| - \|z - v'\|) \end{aligned}$$

Then, for  $\mu < 1/3$  and  $\gamma = \arccos \frac{2\mu}{1-\mu}$ ,

$$\begin{aligned} \|z - a\| - \|z - v'\| &= \frac{\|a-b\|}{2\cos\gamma} - \frac{\|a-b\|}{2} \tan\gamma \\ &= \frac{\|a-b\|}{2} \frac{(1-\mu) - \sqrt{1-2\mu-3\mu^2}}{2\mu} \end{aligned}$$

and

$$\begin{aligned} \delta_v &\geq \left( 1 - \frac{(1-\mu) - \sqrt{1-2\mu-3\mu^2}}{2\mu} \right) \frac{\|a-b\|}{2} \\ &\geq \frac{\sqrt{1-2\mu-3\mu^2} - (1-3\mu)}{2\mu} \frac{\|a-b\|}{2} \end{aligned}$$

□

## Results used to generate sparse $\varepsilon$ -samples

The following result comes from [6]:

**Lemma 6** *Let  $\Sigma$  be a smooth compact surface without boundaries. We call  $d_\tau$  the distance to its skeleton  $\tau$ . Let  $\tilde{X}$  be a set of points on  $\Sigma$ . Assume that  $\forall f \in \text{Del}_\Sigma(\tilde{X})$  every surface Delaunay ball  $B(c_f, r_f)$  of  $f$  is such that  $r_f \leq 0.17 d_\tau(c_f)$ . Then every edge that is incident to a facet of  $\text{Del}_\Sigma(\tilde{X})$  is actually incident to at least two facets of  $\text{Del}_\Sigma(\tilde{X})$ .*

**Lemma 7** Let  $\Sigma$  be a smooth compact connected surface. Let  $\bar{X}$  be an  $\varepsilon$ -sample of  $\Sigma$ , with respect to a given 1-Lipschitz function  $\phi$ . Let  $f_0$  be a facet of  $\text{Del}_\Sigma(\bar{X})$  such that every edge of  $f_0$  is incident to another facet of  $\text{Del}_\Sigma(\bar{X})$ . Call  $X$  the set of vertices of  $f_0$ . Then  $\bar{X} \setminus X$  is a  $\frac{(3+\varepsilon)\varepsilon}{1-\varepsilon}$ -sample of  $\Sigma$ , with respect to  $\phi$ .

**Proof** Let  $x \in \Sigma$ . Let  $v$  be the point of  $\bar{X}$  that is closest to  $x$ . Then  $\|x - v\| \leq \varepsilon \phi(x)$ , since  $\bar{X}$  is an  $\varepsilon$ -sample of  $\Sigma$  with respect to  $\phi$ . Now there are two cases: either  $v \in \bar{X} \setminus X$ , either  $v \in X$ .

- If  $v \in \bar{X} \setminus X$ , then

$$\text{dist}(x, \bar{X} \setminus X) = \|x - v\| \leq \varepsilon \phi(x) \leq \frac{(3+\varepsilon)\varepsilon}{1-\varepsilon} \phi(x)$$

- If  $v \in X$ , then, since every edge of  $f_0$  is incident to another facet of  $\text{Del}_\Sigma(\bar{X})$ , there exists a facet  $f \neq f_0$  that is incident to  $v$ . At least one vertex of  $f$  is not a vertex of  $f_0$ , ie is in  $\bar{X} \setminus X$ . Let  $w$  be such a vertex. By definition,  $(v, w)$  is an edge of  $f$ , ie an edge of  $\text{Del}_\Sigma(\bar{X})$ , thus its dual Voronoi face intersects  $\Sigma$ . Let  $y$  be a point at the intersection. By definition of the Voronoi diagram,  $\|y - v\| = \|y - w\| = \text{dist}(y, \bar{X})$ , which is less than  $\varepsilon \phi(y)$  since  $\bar{X}$  is an  $\varepsilon$ -sample of  $\Sigma$  with respect to  $\phi$ . Thus we have

$$\|y - v\| \leq \varepsilon \phi(y) \leq \varepsilon (\phi(v) + \|y - v\|)$$

ie

$$\|y - v\| \leq \frac{\varepsilon}{1-\varepsilon} \phi(v)$$

Finally, we get

$$\begin{aligned} \text{dist}(x, \bar{X} \setminus X) &\leq \|x - w\| \leq \|x - v\| + \|v - w\| \\ &\leq \|x - v\| + 2 \|v - y\| \\ &\leq \varepsilon \phi(x) + \frac{2\varepsilon}{1-\varepsilon} (\phi(x) + \|x - v\|) \\ &\leq \varepsilon \phi(x) + \frac{2\varepsilon}{1-\varepsilon} (1 + \varepsilon) \phi(x) \\ &\leq \frac{(3+\varepsilon)\varepsilon}{1-\varepsilon} \phi(x) \end{aligned}$$

□

**Lemma 8** Let  $\Sigma$  be a smooth compact connected surface without boundaries. We call  $d_\tau$  the distance to its skeleton  $\tau$ . We have

$$\int_\Sigma \frac{dx}{d_\tau^2(x)} \geq 4\pi$$

**Proof** Let  $d_\tau^{\max} = \max \{d_\tau(y), y \in \Sigma\}$ . We have

$$\int_\Sigma \frac{dx}{d_\tau^2(x)} \geq \frac{\text{Area}(\Sigma)}{(d_\tau^{\max})^2}$$

Since  $\Sigma$  is connected and has no boundary, it bounds an open set  $\Omega$  of  $\mathbb{R}^3$ . Let  $x$  be a point of  $\Sigma$  such that  $d_\tau(x) = d_\tau^{\max}$ . Call  $B_x$  the maximal inner (ie that is included in  $\Omega$ ) ball that is tangent to  $\Sigma$  at  $x$ . Its center is on  $\tau$ , thus its radius is greater than  $d_\tau(x) = d_\tau^{\max}$ . Since  $B_x$  is a ball included in  $\Omega$ , we have

$$\text{Area}(\partial B_x) \leq \text{Area}(\Sigma)$$

which gives

$$4\pi (d_\tau^{\max})^2 \leq \text{Area}(\Sigma)$$

Thus

$$\int_\Sigma \frac{dx}{d_\tau^2(x)} \geq 4\pi$$

□

## References

- [1] P. Agarwal and S. Suri. Surface approximation and geometric partitions. *Proc. 5th Annu. ACM Sympos. Discrete Algorithms*, 1994. pp 24-33.
- [2] P. Alliez, E. Colin de Verdière, O. Devillers and M. Isenburg. Isotropic Surface Remeshing. *Solid Modelling and Applications*, 2003.
- [3] N. Amenta and M. Bern. Surface Reconstruction by Voronoi Filtering. *Proc. 14th Annu. ACM Sympos. Comput. Geom.*, 1998, pp 39-48.
- [4] D. Attali, J-D Boissonnat and A. Lieutier. Complexity of the Delaunay Triangulation of Points on Surfaces: the Smooth Case. *Proc. 19th Annu. ACM Sympos. Comput. Geom.*, 2003.
- [5] J-D Boissonnat and F. Cazals. Natural Neighbour Coordinates of Points on a Surface. *Comp. Geom. Theory and Appl.*, 155-174, 2001.
- [6] J-D Boissonnat and S. Oudot. Restricted Delaunay Triangulation and Point Samples. Manuscript, available upon request.
- [7] E. V. Chernyaev. Marching Cubes 33: Construction of Topologically Correct Isosurfaces. Technical report CERN CN 95-17, 1995.
- [8] L. P. Chew. Guaranteed-Quality Mesh Generation for Curved Surfaces. *Proc. 9th Annu. ACM Sympos. Comput. Geom.*, 1993, pp 274-280.
- [9] M. Desbrun, N. Tsingos and M-P Gascuel. Adaptive Sampling of Implicit Surfaces for Interactive Modeling and Animation. *Proc. Implicit Surfaces*, pp 171-185, 1995.
- [10] O. Devillers. Improved incremental randomized Delaunay triangulation. *Proc. 14th Annu. ACM Sympos. Comput. Geom.*, pp 106-115.
- [11] H. Edelsbrunner, N.R. Shah. Triangulating topological spaces. *International Journal of Computational Geometry and Applications*, Vol. 7, No. 4 (1997), pp 365-378.
- [12] J. Erickson. Nice point sets can have nasty Delaunay Triangulations. *Proc. 17th Annu. Sympos. Comput. Geom.*, pp 96-105, 2001.
- [13] I. Guskov, W. Sweldens and P. Schröder. Multiresolution Signal Processing for Meshes. *Proc. SIGGRAPH*, pp 325-334, 1999.
- [14] J. Hart and B. T. Stander. Guaranteeing the Topology of an Implicit Surface Polygonization for Interactive Modeling. *Proc. SIGGRAPH*, 1997.
- [15] H. Hoppe, T. DeRose, T. Duchamp, J. McDonald and W. Stuetzle. Mesh Optimization. *Proc. SIGGRAPH*, pp 19-26, 1993.
- [16] K. Hormann, U. Labsik and G. Greiner. Remeshing Triangulated Surfaces with Optimal Parameterizations. *Computer-Aided Design* 33, pp 779-788, 2001.
- [17] K. Hormann, U. Labsik, M. Meister and G. Greiner. Hierarchical Extraction of Iso-Surfaces with Semi-Regular Meshes. *Solid Modelling and Applications*, 2002.
- [18] W. E. Lorensen and H. E. Cline. Marching Cubes: a High-Resolution 3D Surface Construction Algorithm. *Proc. SIGGRAPH*, 1987.
- [19] S. A. Mitchell. Cardinality bounds for triangulations with bounded minimum angle. *Proc. 6th Annu. Canadian Conference Comput. Geom.*, pp 326-331, 1994.

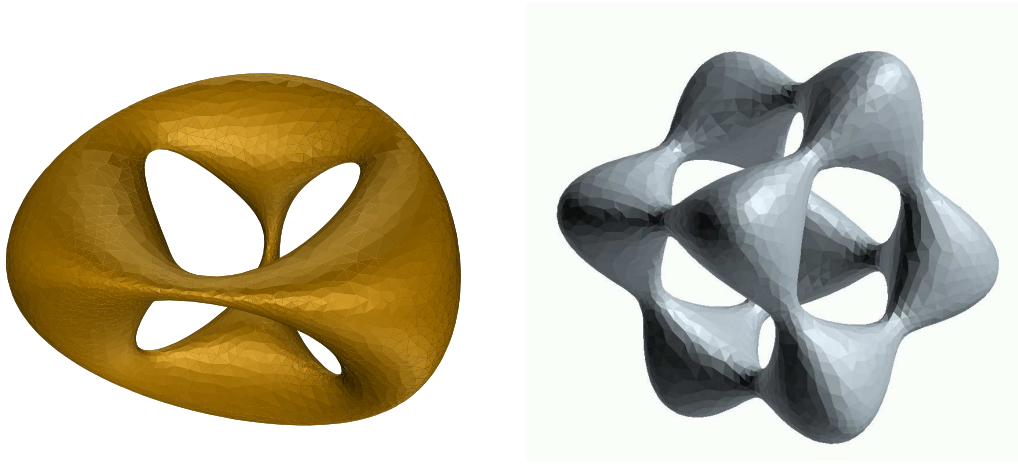


Figure 5: Smooth implicit surfaces.

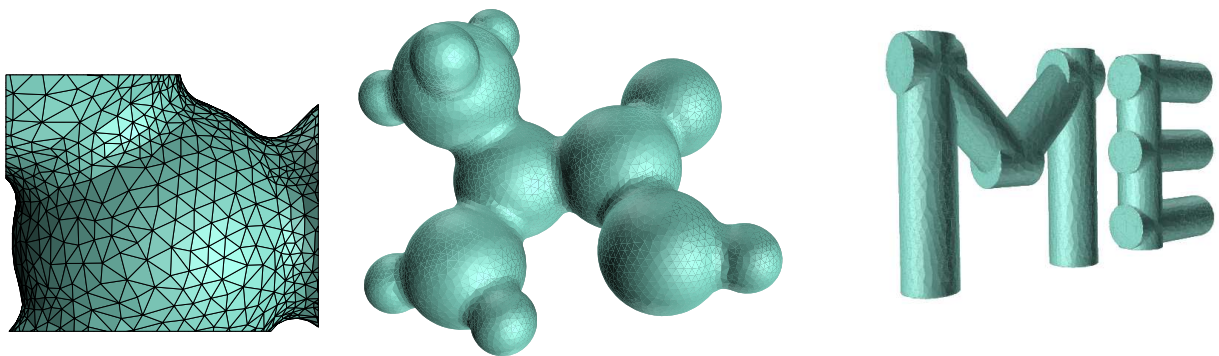


Figure 6: Examples from biogeometry (left and center) and CAD (right).

- [20] J-M Morvan and B. Thibert. On the Approximation of the Area of a Surface. INRIA RR-4375, 2002.
- [21] J. Ruppert. A Delaunay Refinement Algorithm for Quality 2-Dimensional Mesh Generation. *Journal of Algorithms*, May 1995.
- [22] J. R. Shewchuk. Delaunay Refinement Algorithms for Triangular Mesh Generation. *Comput. Geom. Theory & Applications*, 22(1-3):21-74, may 2002.
- [23] G. Turk. Generating Textures for Arbitrary Surfaces using Reaction-diffusion. *Proc. SIGGRAPH*, pp 289-298, 1991.
- [24] G. Turk. Re-tiling Polygonal Surfaces. *Proc. SIGGRAPH*, pp 55-64, 1992.
- [25] A. Witkin and P. Heckbert. Using Particles to Sample and Control Implicit Surfaces. *Computer Graphics*, pp 269-278, 1994.

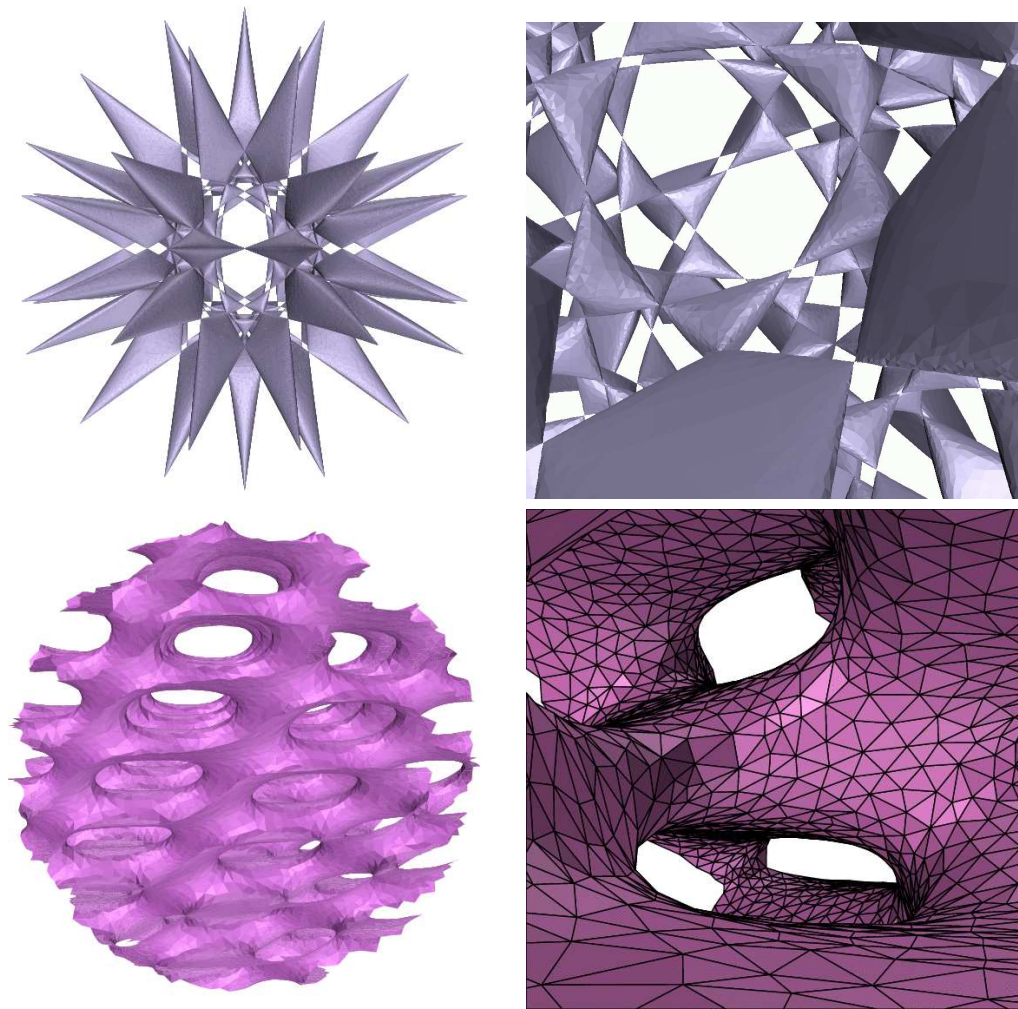


Figure 7: Barth's decic and Sheffer's surfaces.

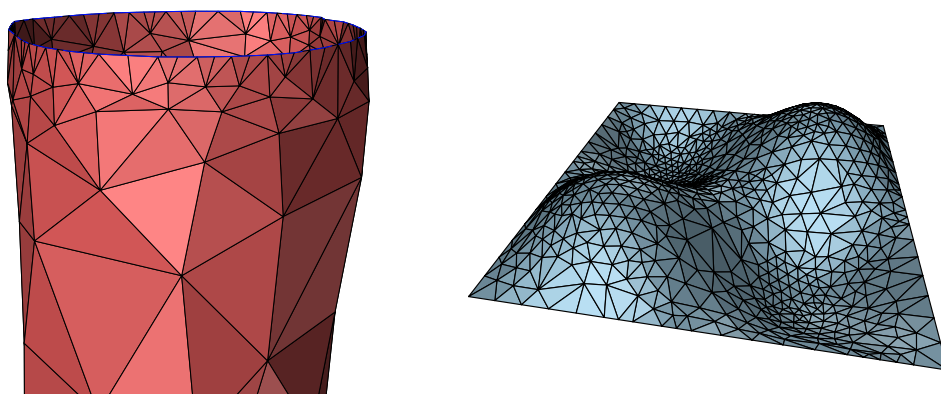


Figure 8: Dealing with boundaries.

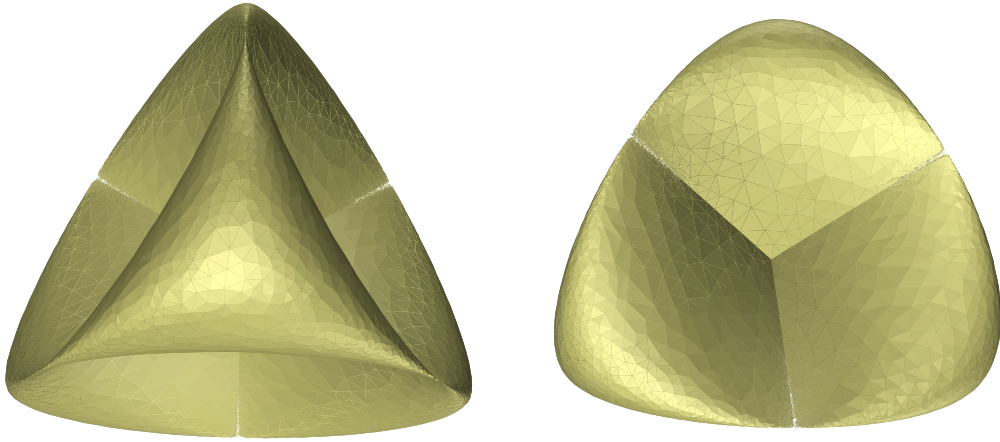


Figure 9: Dealing with singularities.

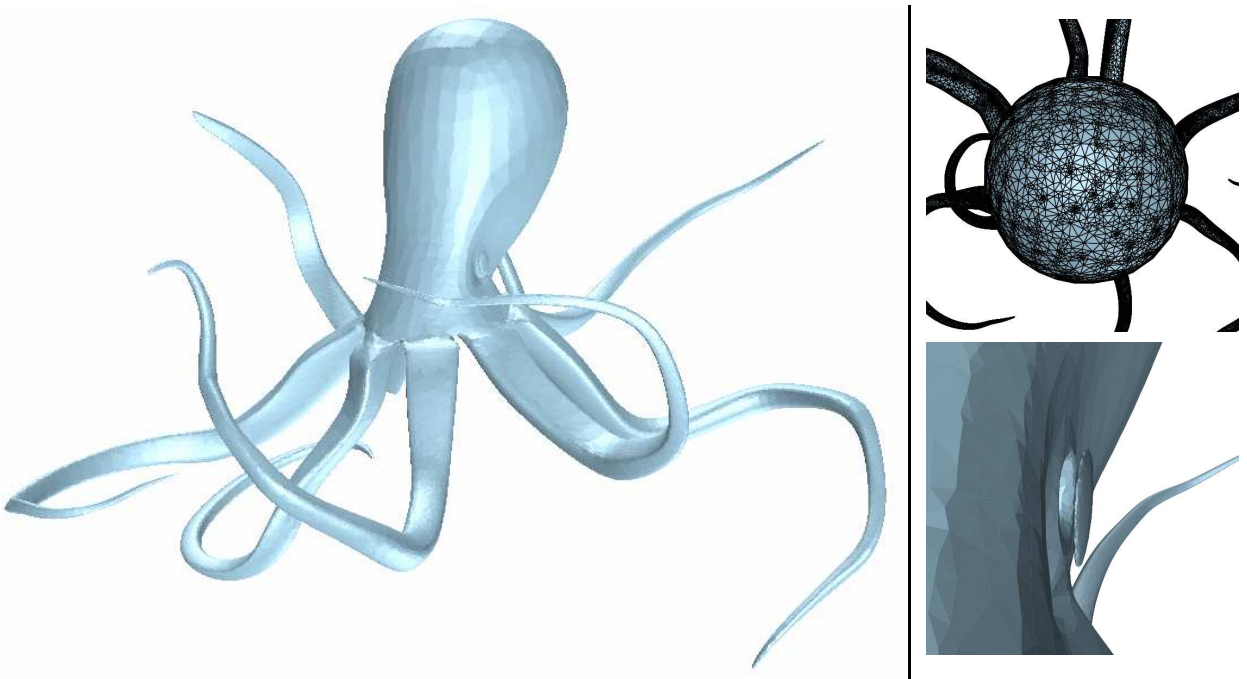


Figure 10: Polyhedron remeshing.